J Mater Sci: Mater Electron (2014) 25:4348–4355
DOI 10.1007/s10854-014-2172-z

Heat transfer in photonic mirrors

D. Estrada-Wiese · J. A. del Río · M. B. de la Mora

Received: 21 June 2013 / Accepted: 11 July 2014 / Published online: 29 July 2014

Abstract The use of secondary mirrors in solar energy concentration is common. However, high concentrated solar radiation heats these mirrors thereby degrading their physical properties. In particular, aluminum mirrors melt because of high temperature due to storage by high radiative heat transfer. In contradistinction photonic crystals could present "perfect reflection" and they can be fabricated using porous silicon which has a higher melting point than aluminum (porous silicon has a melting point higher than 900 K). Porous silicon is a nanostructured semiconductor material which can be fabricated with different porosities and refractive indices. Multilayers of alternating periodic refractive index conform the structure of these photonic crystals. The light that propagates in these structures interacts with its periodic refractive index that generates wavelength gaps of forbidden transmission and so these multilayers conform a mirror. Even these photonic structures are heated when they are exposed to high concentrated solar radiation. In this work we experimentally analyze this heating process and model it using an effective medium approach to explain the increasing temperature behavior.

D. Estrada-Wiese (✉) · J. A. del Río
Instituto de Energías Renovables, Universidad Nacional Autónoma de México, Privada Xochicalco S/N, 62580 Temixco, Morelos, Mexico
e-mail: de.e.wiese@gmail.com

M. B. de la Mora
Departamento de Ingeniería de Procesos e Hidráulica, División de Ciencias Básicas e Ingeniería, Universidad Autónoma Metropolitana-Iztapalapa, Av. San Rafael Atlixco 186, Col. Vicentina, Del. Iztapalapa, D.F. 09340, Mexico

1 Introduction

Day after day society is more convinced about the need to use renewable energy sources. Solar energy is one of such sources as it is free, clean and inexhaustible. For this reason it is so important to develop technology in solar concentration devices. They are used to produce electrical power, light transmission through optical fibers for room lighting [1], and industrial process heat applications [2], amongst others. A solar concentration system consists of an array of mirrors and an absorber. In order to simplify the structure and avoid ray obstruction a secondary reflector is used. Photonic mirrors made of porous silicon (p-Si) multilayers are suitable for this purpose, due to their optical properties and high reflectivity [3]. Alternating layers of material with different refractive indexes are the simplest photonic crystals known. These periodic dielectric films in a Bragg structure act as a mirror. It is possible to fabricate p-Si mirrors of high quality, however it has been shown by de la Mora et al. [3] that despite their high reflectivity p-Si mirrors absorb radiation and have an increase in temperature. In that study an aluminum mirror to one made of p-Si was compared, recording temperature with a K-type thermocouple on the internal surface of the samples. They found that the p-Si mirror reached temperatures beyond 900 °C and observed sample degradation. Since Al has a lower melting point than silicon it degrades more easily than the p-Si mirror. We acknowledge that there is a limitation in the experiment that was carried out by the group of de la Mora: the use of a thermocouple makes an indirect measurement of temperature. We consider that an alternative way of measuring temperature has to be found.

Many studies have been done on optical properties of this material [4–10], but it is necessary to understand how heat is transported in a p-Si multilayer structure. Using

experimental methods like 3 ω [11, 12] or photoacustic tecnique [13], some thermal properties of p-Si have been studied. Thermal conductivity has been measured by using indirect measurement of temperature. This is the reason we have implemented the use of an infrared camera as a different method for temperature measurement.

In this work we design and fabricate high reflective p-Si multilayer mirrors, heat them up using concentrated solar radiation, and study heat propagation on them. In order to compare the quality of our mirrors we measure temperature changes in different mirrors: aluminized silicon (Si-Al), standard mirror (a secondary surface aluminized glass) named "Al mirror" and electropolished silicon wafer (c-Si). We use an easy approach to calculate effective thermal properties in multilayer structures. The results of these calculations are used to analyze and interpretate our experimental temperature profiles.

This paper is organized as follows: In Sect. 2, the fabrication procedure of p-Si multilayers and the reflectance spectrum of the mirrors are presented. In Sect. 3, a theoretical method to calculate effective thermal properties in compound media is used to obtain the thermal diffusivity of p-Si multilayers. This is based on a formula developed by del Río et al.[15], using effective media fitting. With this technique we obtain values for effective thermal diffusivity of our p-Si multilayer. Considering that the other mirrors are composed by layers we use standard series heat transfer calculations. In Sect. 4, the experimental procedure to heat up the mirrors is described. Then, we explain the use of an infrared camera to measure temperature in the heated samples. In Sect. 5, we show our findings and discuss them in terms of our theoretical framework. Finally, we state some conclusions about our work.

2 Fabrication of p-Si multilayers

Porous silicon can be produced by using electrochemical etching of crystalline silicon in a hydrofluoric acid (HF) solution. The electrolyte is composed of ethanol, HF and glycerol at a volume ratio of 7:3:1, respectively. Anodization begins when a constant current between the electrolyte and the Si wafer, in our case type p (resistivity of 0.1–0.02 Ω cm and (100) orientation) is applied. By alternating the current density between 1.5 and 40 mA/cm^2, layers of low and high porosity, 15 and 56 % [14], can be produced. Consequently, the layers present different refractive indices with values of 2.4 and 1.4, respectively (Fig. 1).

The structure of a p-Si multilayer is composed of a continuous arrangement of submirrors. Each mirror is designed to reflect a different wavelength λ and consist of 5 periods. Values for λ are chosen as follows: first the initial value λ_1 is given, the other values will follow the relation: $\lambda_{i+1} - \lambda_i = 2i\frac{\lambda_n - \lambda_1}{n(n+1)}$, where i represents the submirror number and n the total number of submirrors.Our multilayer is composed of 20 submirrors, of 5 periods each, with a total width of 68.8 $\times$ 10^3 nm. By designing multilayers with these properties we are able to fabricate mirrors which reflect a continous range of the electromagnetic spectrum.

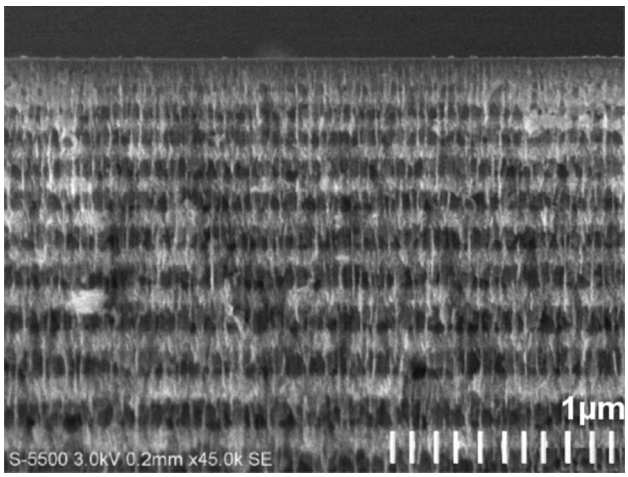

Fig. 1 SEM transversal section image of a p-Si multilayer part, fabricated in porous silicon lab at IER, UNAM

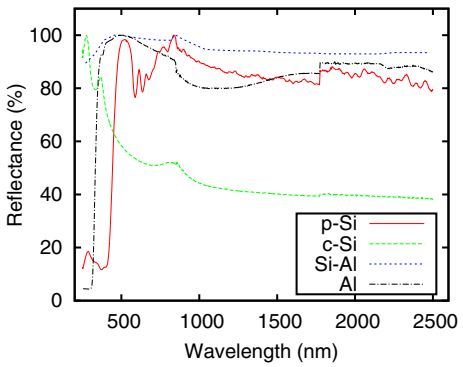

Fig. 2 Experimental reflectance spectrum of our p-Si (*red continuous line*), c-Si (*green dashed line*),Si-Al (*blue dotted line*) and Al mirror (*black dashed lines with dots*) (Color figure online)

Our mirror was designed to reflect light from the visible to the near infrared (500–2,500 nm). To measure the reflectance of the samples a spectrophotometer UV–Vis-IR (Shimadzu UV1601) was used. The corresponding spectra for different reflectant surfaces, used in our experiments, are shown in Fig. 2. For these results it is clear that they are mirrors with high reflectivity, that can be used as secondary mirrors under high concentrated solar radiation. In the next section we explain the effective medium approach we use to calculate thermal diffusivity.

3 Effective thermal conductivity in porous silicon multilayers

Heat transfer in porous materials can be described by effective media approaches. The values of effective thermal properties in compound materials can be obtained when using effective methods. Using the formula for conductivity in a material of two components [15], the thermal effective conductivity, and effective specific heat of one layer of p-Si has been calculated by Eq. 1. This expression satisfies Keller's reciprocity condition at all values of the concentration. It is useful to obtain values for average physical properties in composite materials where the microstructure is very dependent on the preparation conditions.

The effect of nonconstant transport coefficients produce nonlinear contributions. Studies show that only in special cases the nonlinear terms are important, then the temperature dependence of the local conductivities can be neglected [16]. In general, it is a good approximation to use the local conductivities as constant in order to calculate the effective thermal conductivity. The calculations throughout the study are therefore purely qualitative; in order to get a direct approximation it is necessary to take into account temperature dependency [17].

$$\kappa_{eff} = \kappa_1 \frac{1 + c(\sqrt{\frac{\kappa_2}{\kappa_1}} - 1)}{1 + c(\sqrt{\frac{\kappa_1}{\kappa_2}} - 1)} \tag{1}$$

Here we use $\kappa_1 = 148\ \frac{W}{K \cdot m}$ as the thermal conductivity of silicon and $\kappa_2 = 0.024\ \frac{W}{K \cdot m}$ of air [21]. Effective thermal conductivity in p-Si has been calculated considering the porosity of one layer of p-Si as the concentration (c). For our periodic structure of layers of high (56 %) and low (15 %) porosity, κ_{eff} for each layer (named 1 and 2) was calculated, obtaining values of $\kappa_{eff_1} = 1.489\ \frac{W}{K \cdot m}$ and $\kappa_{eff_2} = 9.972\ \frac{W}{K \cdot m}$, respectively. We notice that κ_{eff_1} and κ_{eff_2} have smaller values than κ_1, the thermal conductivity of silicon. Layers of p-Si are less conductive than silicon as their conductivity depends on the porosity of the material.

3.1 Effective specific heat

Effective specific heat at constant pressure was calculated in an analogous form as $\kappa_e ff$. Using Eq. 1 for $\rho_1 c_{p_1}$, where c_p is the specific heat at constant pressure and ρ is the density of p-Si. While $\kappa_2 = \rho_2 c_{p_2}$ is the analogous for air.

$$\rho c_{p_{eff}} = \rho_1 c_{p_1} \frac{1 + c(\sqrt{\frac{\rho_2 c_{p_2}}{\rho_1 c_{p_1}}} - 1)}{1 + c(\sqrt{\frac{\rho_1 c_{p_1}}{\rho_2 c_{p_2}}} - 1)}. \tag{2}$$

We use the following values to determine effective specific heat for each layer, being $\rho_1 = 2{,}330\ \text{kg/m}^3$ and $c_{p_1} = 700$ J/kg K [3] density and specific heat for crystalline silicon; such as $\rho_2 = 1.05\ \text{kg/m}^3$ and $c_{p_2} = 1{,}012$ J/kg K for air [21]. Using Eq. 2, with the proper concentration values for each layer, we obtain values of $\rho_1 c_{p_{eff1}} = 33'111.45\ \frac{\text{J}}{\text{m}^3\text{K}}$ for high porosity layer and $\rho_2 c_{p_{eff2}} = 207'024.49\ \frac{J}{m^3 K}$ for the low porosity ones. From here we see that the effective values of porous silicon are smaller than $\rho_1 c_{p_1} = 1'631'000\ \frac{J}{m^3 K}$. More heat is needed to increase the temperature of p-Si layers than ordinary silicon layers.

3.2 κ_{eff} and $\rho_t c_{p_{eff}}$ of p-Si multilayer

A submirror of p-Si is formed of $\frac{n}{2}$ periods of different porosities as can be seen in Fig. 3. Each layer has a width d_1 and d_2 respectively, being a the total width of the submirror. We use a formula to describe the effective conductivity for a p-Si submirror, in which we assume that

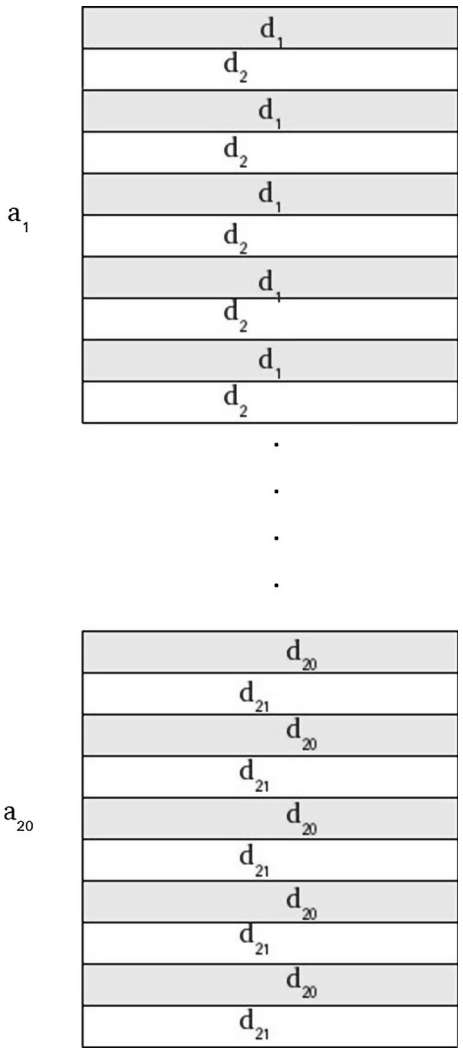

Fig. 3 Scheme of the structure of submirrors in the multilayer, where a_i is the width of each layer

the heat is transported in a tranvers way to the layers, which in our case are paralell. In a general way we have

$$\mathbf{K} = \frac{n}{2}\frac{(k_{eff_1}d_1 + k_{eff_2}d_2)}{a}, \tag{3}$$

where k_1 is the effective conductivity in the first layer and k_2 in the second. To find the total effective conductivity of the multilayer, we consider 20 submirrors, each one with 5 periods, meaning 5 layers of width d_i , κ_{eff_i} and $\rho_i c_{p_{eff_i}}$ and 5 layers of width d_{i+1}, $\kappa_{eff_{i+1}}$ and $\rho_{i+1}c_{p_{eff_{i+1}}}$. Where $i = 1\ldots r$, represents the number of submirrors. In Fig. 3, a scheme of the structure of the p-Si multilayers is shown.

We use Eq. 3 to find κ_{eff} or $\rho_{c_{p_{eff}}}$ of each submirror. To calculate the total effective conductivity of the multilayer, the next relation is used:

$$K_{eff_m} = \frac{k_1a_1 + k_2a_2 + \cdots + k_{20}a_{20}}{a_1 + a_2 + \cdots + a_{20}}, \tag{4}$$

where a_i is the width and k_i is the effective conductivity of each submirror, $i = 1, 2, \ldots, 20$.

Our p-Si multilayer is not freestanding, namely it is over the crystalline silicon substrate. In order to calculate the total effective conductivity, we need to consider the substrate of c-Si as the last layer of the structure. From Eq. 4, we consider only two elements: the p-Si multilayer and c-Si wafer

$$K_{m_{total}} = \frac{k_m a_m + k_{c-Si}a_{c-Si}}{a_m + a_{c-Si}}. \tag{5}$$

Here k_m, is the effective conductivity of the multilayer, k_{c-Si} of crystalline silicon and a_m and a_{c-Si} the width of each layer.

Using Eq. 4 and 5, we find values for effective thermal properties in our multilayer of porous silicon, and the other studied mirrors. The Al mirror is made of a very thin layer of aluminum (1.5×10^6 m) covered with a thick glass of width 3×10^{-3} m. The c-Si wafer, aluminized silicon and p-Si mirror have all the same width (1×10^{-3} m). The results are shown in Table 1 where the criterion of significant figures was used. For discussion we also present a free-standing p-Si multilayer, which can be prepared as described in the literature [18].

Notice that the capacity of heat transfer in c-Si sample is higher than in the p-Si multilayer. The difference between the values of a freestanding sample of p-Si and c-Si are very high, establishing that heat transfer in a porous media, such as p-Si is higher than in other materials such as c-Si. The capacity to dissipate thermal energy relates to a lower temperature increase. Regarding earlier discussion we can confirm that p-Si is a good candidate as a thermal insulator [19, 20]. Now we intend to compare the results obtained from our calculations with the experiment. In the next section we present how this experiment was carried out.

4 Experimental procedure

In what follows, we describe the experiments performed to study heat propagation in a p-Si mirror, a silicon wafer, an aluminum mirror (Al), and an aluminized silicon wafer. In order to compare all the samples, we exposed them simultaneously under solar radiation. Then we studied temperature change in each one.

Our experimental arrangement consisted of a magnifying glass (Ergologic, 75 mm ϕ, 3×) used to concentrate solar radiation of the samples, reducing the diameter of the Sun image to 5×10^{-3} m. Although we did not measure irradiance we do know it is the same for all the samples. The magnifying glass was held at a universal support paralell to the mirrors at 7 cm distance, so the light would fall normal upon them. The mirrors were supported by crocodile clips covered with tape to avoid heat flux to the support. To measure temperature change on the samples an infrared camera (Flir T-300)[22] was placed next to the mirrors. In order to perform the role of noncontact temperature recorder, the camera will change the temperature of the measured object depending on the camera settings. We used the next camera adjustment parameters: emissivity: 0.95, distance: 0.3 m, reflected temperature: 20 °C, room temperature: 27 °C and humidity: 27 °C. Emissivity was determined using the "Adjacent Spot" method, described in [23]. Our mirrors reflected radiation from the sky and surroundings, which competed strongly with the radiation emition due to its temperature. If these aspects

Table 1 Values for width, thermal conductivity, effective specific heat and effective thermal diffusivity of the samples

Sample	$a\,(m)$	$\kappa_{\mathbf{eff}}\left(\frac{W}{K\cdot m}\right)$	$\rho\mathbf{c}_{\mathbf{p}_{eff}}\left(\frac{J}{K\cdot m^3}\right)$	$\alpha_{\mathbf{eff}}\left(\frac{m^2}{s}\right)$
Free-standing p-Si multilayer	6.88×10^{-5}	3.18	685×10^2	4.64×10^{-5}
p-Si multilayer + c-Si	1.068×10^{-3}	138.67	153×10^4	9.06×10^{-5}
Crystalline silicon	1.0×10^{-3}	148.0	163×10^4	9.07×10^{-5}
Aluminum mirror	3.0015×10^{-3}	0.914	207×10^4	4.40×10^{-7}
Aluminized silicon	1.0×10^{-3}	148.06	163×10^4	9.07×10^{-5}

interfere with the measurements made with the IR camera, then we knew we needed to avoid reflections. In order to block radiation from surroundings, we placed a screen next to the samples.

IR images were taken during the heating of the mirrors indicating a significant temperature increase. These were analized using the "ThermaCAM Researcher Professional 2.1" software as follows. The temperature was measured in two different ways:

- Selecting the central "Spot" of each sample, and defining the temperature at the same point in all the images of the experimental series.
- Selecting an area (circle) that includes each mirror and estimating the average temperatures of the mirrors in each image sequence.

The thermal response of the p-Si mirror and the comparison with other mirrors is shown in the next section.

5 Temperature evolution under concentrated radiation

Heat transfer in a p-Si multilayer mirror was measured using an infrared camera. IR images were taken to measure temperature in the mirror after aprox. 4–5 min of exposure to concentrated solar radiation. Timeslots were measured using a chronometer. The results show a significant temperature increase despite the high reflectance of the sample.

We ploted temperature within time on the sample, see Fig. 4.

Measurements show a temperature increase of 30 °C over environmental temperature, reaching a final temperature of 70 °C. It is important to mention that during some experiments wind appears, as can be observed around 30 s in Fig. 4. After showing that a dielectric mirror absorbs energy and therefore increases its temperature, we compared our photonic structure with other mirrors: a conventional Al mirror and a c-Si wafer. It is important to note

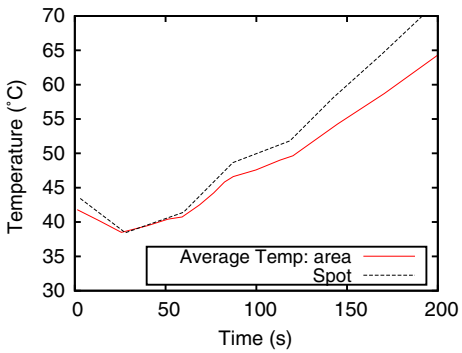

Fig. 4 Temperature measurement in Spot (same point), and Area versus time in p-Si mirror

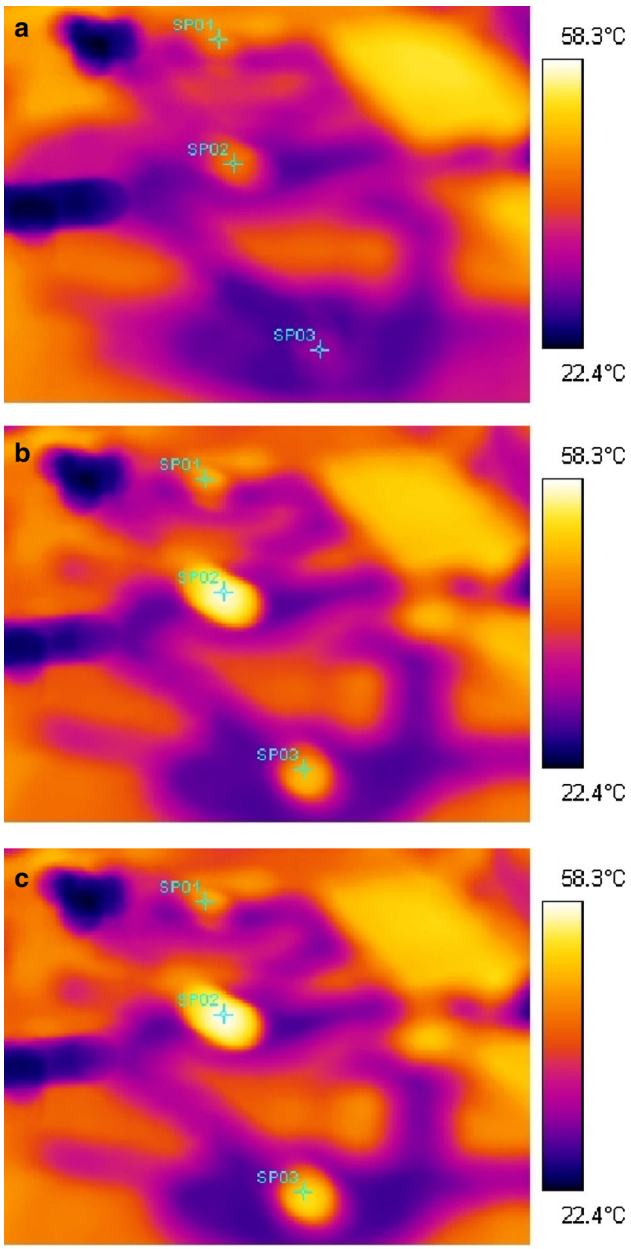

Fig. 5 IR Image at time **a** t = 0 min, **b** t = 2 min, **c** t = 4 min

that the Al mirror is three times more massive than the other samples, consequently we expect less temperature increase for this mirror. Figure 5 shows IR images of the initial, intermediate and final measurements of the experimental session. These IR images show a visual display of the amount of infrared energy emitted, transmitted and reflected by our samples. Using a series of mathematical algorithms the camera builds a picture in the visible range allowing us to represent temperature variations by associating colors to temperature values. We are therefore able to detect the warmer areas in the image where the samples are being heated. Note that the samples are placed over a

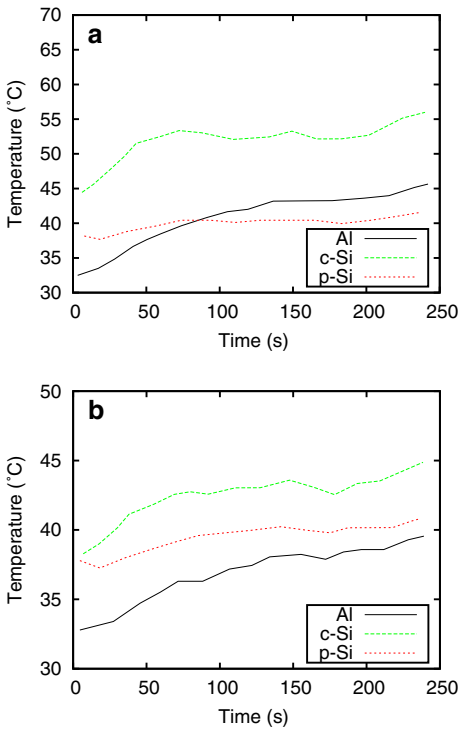

Fig. 6 **a** Temperature measurement versus time in spot, **b** Average temperature versus time in area of three mirrors: aluminum mirror (*black continous line*), silicon wafer (*green dashed line*) and porous silicon (*red dotted line*) (Color figure online)

fabric, which is not completely flat, it then absorbs and emits radiation in a different way depending on the region. The mirrors are distributed in descending order of the IR images, starting with the p-Si, then the c-Si and at last the Al mirror.

The results of the temperature measurement of the samples, as seen in Fig. 6, show a temperature increase in the three mirrors. Several measurements (10) were made showing the same typical behavior, fluctuating only because of climatic factors like wind or incident radiation.

Crystalline silicon is the sample that heat up the most, reaching temperatures of 57 °C. P-Si did not increase its temperature as much, with an initial value of 37 °C it heat up to 42.4 °C. The aluminum mirror is the sample that had the most temperature difference, with an initial temperature of 31.9 °C and a final of 45.3 °C.

It is important to mention that the initial values of the samples differ from each other due to an experimental complication: The magnifying glasses were covered to block solar radiation on the samples before measurements were made. Because of the difficulty to uncover all three mirrors at the same time to expose them to solar radiation and begin with the measurements, the samples were heated one to two seconds apart, therefore the initial temperature response is different.

In order to present results independent of those initial conditions and considering our calculations for effective diffusivity, we now show temperature evolution by removing the initial temperature of each sample and dividing between α_{eff_j}, where j stands for each sample.

From Fig. 7 we can infer that our p-Si sample dissipates heat much better than the Al and c-Si mirrors. Comparing this result with Fig. 6 it is clear that the diffusivity of each sample plays an important role in heat transfer in mirrors, hence it can not be ignored. The aluminum mirror seemed to be a better reflector than our p-Si sample, but considering the thermal properties of the material, we have shown the opposite.

As we mentioned previously, we fabricated an aluminized silicon (Si-Al) mirror through evaporation. This mirror has the same width and superficial area than our p-Si mirror. For comparative results this mirror is more convenient, therefore we exchanged the Al mirror for the Si-Al wafer. Measurements are made the same way as before. Results are shown in Figs. 8 and 9. The same temperature behavior in the p-Si and c-Si samples is observed, the aluminized silicon has less temperature increase than the other mirrors.

The results shown in Figs. 6 and 8 indicate the temperature increase in all the mirrors. The temperature

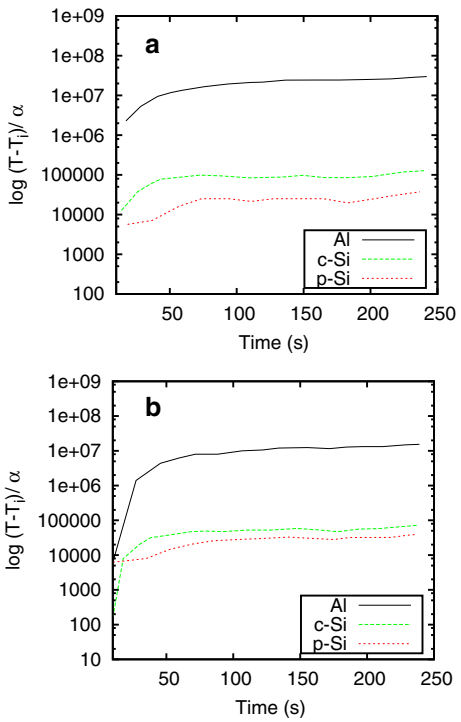

Fig. 7 **a** Temperature measurement in spot: $\Delta T/\alpha_{eff_j}$ for each sample, **b** Average temperature versus time, $\Delta T/\alpha_{eff_j}$, in area of three mirrors: aluminum mirror (*black continous line*), silicon wafer (*green dashed line*) and porous silicon (*red dotted line*) (Color figure online)

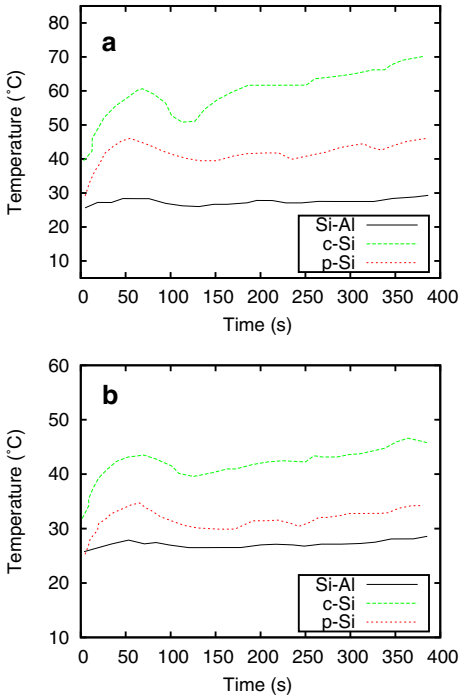

Fig. 8 **a** Temperature measurement versus time in spot, **b** Average temperature versus time in area of mirrors: aluminized silicon (*black continous line*), silicon wafer (*green dashed line*) and porous silicon (*red dotted line*) (Color figure online)

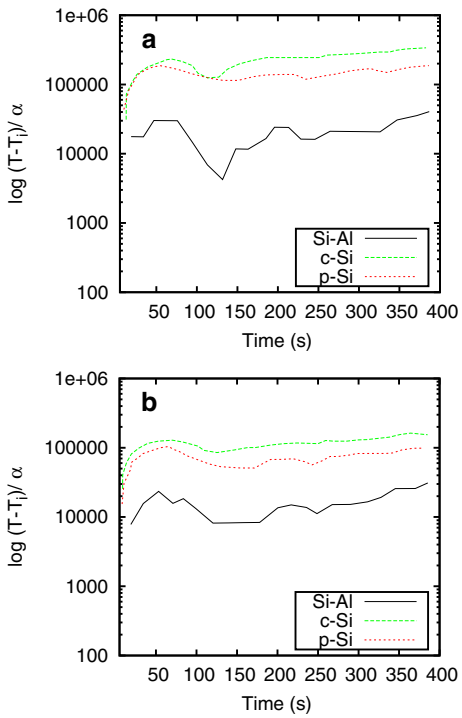

Fig. 9 **a** Temperature measurement in spot, $\Delta T/\alpha_{eff_i}$, of mirrors: aluminized silicon (*black continous line*), silicon wafer (*green dashed line*) and porous silicon (*red dotted line*) **b** Average temperature versus time in area $\Delta T/\alpha_{eff_i}$ of samples (Color figure online)

changes are different for the four types of mirrors, however we can explain these differences. From our calculations in Sect. 3.2 and summarized in Table 1, we find the following relation: $\alpha_{eff_{Almirror}} < \alpha_{eff_{free-standingp-Si}} < \alpha_{eff_{p-Si}} < \alpha_{eff_{c-Si}} = \alpha_{eff_{Si-Al}}$; this implies that the Si-Al dissipates the absorbed radiation more efficiently in addition to heating up less. Although the c-Si and Si-Al present similar values, we observed that Si-Al does not present a great temperature increase. This can be related to the high reflectivity of the Si-Al mirror (see Fig. 2) that lets the mirror absorb less radiation than the c-Si one. The sample that contradicts our calculations is cristaline silicon, which has the same value of α_{eff} as Si-Al but a much larger temperature increase. This is also explained by considering its reflectance spectrum. C-Si has low reflectivity, absorbs more radiation and heats up more.

We are not able to compare experimental and theoretical results for a free-standing p-Si multilayer because of the lack of experimental data. Free-standing samples are very fragile and break easily, making them difficult to handle. This is an experimental challenge that we will continue to face in the future.

6 Conclusions and remarks

Photonic crystals as secondary mirrors have been used in concentrated solar energy applications; although they present heating which degradates their optical properties [3]. In this study we gathered new information about heat transfer in photonic crystals. We fabricated a photonic crystal of porous silicon multilayers and compared it to a silicon wafer, a standard aluminum mirror and an aluminized silicon wafer. An infrared camera was used to measure temperature change when the samples were under concentrated solar radiation. Furthermore we proposed an easy method to calculate effective thermal properties in compound materials, such as porous silicon. Then we used these values combined with our experimental data to explain the increasing temperature behavior in the samples. As we are studying mirrors the reflectance spectrum was also measured and found that it is very important to consider wavelength dependence on the reflectivity. We concluded that aluminized silicon is the mirror that has the highest reflectivity and the greatest effective thermal diffusivity. Our p-Si mirror is almost as reflective as Si-Al, however it has a smaller value of α_{eff} and showed a greater temperature increase. Although the Si-Al loses its properties to a lower temperature [3]. One of the challenges we will face in the future is to fabricate better and more reflective porous silicon mirrors in order to compete with the Si-Al. We also made calculations for a freestanding sample of porous silicon multilayer; the value obtained is

smaller than the one of our p-Si mirror. With these calculations from effective media approximation we can describe the thermal properties of photonic crystals prepared with porous silicon.

Acknowledgments We acknowledge useful discussions with Dr. J. Tagüeña Martínez and J. Campos for providing SEM images. Work partially supported by PAPIIT IN 109812 and CONACYT under grant 133763.

References

1. H. Abdul-Rahman, C. Wang, Am. J. Environ. Sci. **6**, 428–437 (2010)
2. S. Kalogirou, Appl. Energ. **74**, 337–361 (2003)
3. M.B. de la Mora, O.A. Jaramillo, R. Nava, J. Tagüeña Martínez, J.A. del Río, Sol. Energ. Mat Sol. C. **93**, 1218–1224 (2009)
4. M.C. Arenas, Hailin Hu, R. Nava, J.A. del Río, Int. J. Modern Phys. B. **24**, 4835–4850 (2010)
5. O. Bisi, S. Ossicini, Pavesi, Surf. Sci. Rep. **38**, 1–126 (2000)
6. M. B. de la Mora. Tesis doctoral en Ingeniería y Ciencias de Materiales. UNAM (2011)
7. V. Agarwal, J.A. del Río, Int. J. Modern Phys. B. **10**, 99–110 (2006)
8. V. Agarwal, J.A. del Río, Appl. Phys. Lett. **82**, 10 (2003)
9. A.G. Palestino, M.B. de la Mora, J.A. del Río, C. Gergely, E. Pérez, Appl. Phys. Lett. **91**, 1219091–3 (2007)
10. M.E. Calvo, S. Colodrero, N. Hidalgo, G. Lozano, C. López-López, O. Sánchez-Sobrado, H. Míguez, Energ. Environ. Sci. Adv. Article (2011)
11. J. De Boor, D.S. Kim, X.AgD Hagen, A. Cojocaru, H. Föll, V. Schmidt, EPL **96**, 16001 (2011)
12. G. Gesele, J. Linsmeier, V. Fricke, R. Arens-Fischer, J. Phys. D. Appl. Phys. **3**, 2911–2916 (1997)
13. A. Gutierrez, J. Giraldo, M.E. Rodríguez-García, Rev. Mex. Fis. **57**, 99–105 (2011)
14. R. Nava, M. B. de la Mora, J. Tagüeña Martínez, J.A del Río. Phys. Status Solid C, 1–4 (2009)
15. J.A. del Río, R.W. Zimmerman, R.A. Dawe, Solid State Commun. **106**, 183–186 (1998)
16. J.E. Lugo, J.A. del Río, J. Tagüeña-Martínez, Trans. Porous. Med. **31**, 89–108 (1998)
17. G. Gesele, J. Linsmeier, V. Drach, J. Fricke, R. Arens-Fischer, J. Phys. D. Appl. Phys. **30**, 2911–2916 (1997)
18. Y. Kanemitsu, H. Uto, Y. Masumoto, T. Matsumoto, T. Futagi, H. Mimura, Phys Rev. B. **48**, 2827–2830 (1993)
19. S. Périchon, V. Lysenko, Ph Roussel, B. Remaki, B. Champagnon, D. Barbier, P. Pinard, Sensor. Actuator. **85**, 335–339 (2000)
20. V. Lysenko, V. Gliba, V. Strikha, A. Dittmar, G. Delhomme, Ph Roussel, D. Barbier, N. Jaffrezie-Renault, C. Martelet, Appl. Surf. Sci. **123**(124), 458–161 (1998)
21. W. M. Haynes, Handbook of Chemistry and Physics, 94th edn, (CRC 2013–2014), http://www.hbcpnetbase.com/
22. FLIR, Technical Data Flir T300, http://support.flir.com/DsDownload/Assets/45305-0201_en_50
23. FLIR, The Ultimate Infrared Handbook For R & D Professionals, http://www.flir.com/uploadedFiles/Thermography/MMC/Brochures/T559243/T559243_APAC